Photochemical & Photobiological Sciences

PAPER

Cite this: *Photochem. Photobiol. Sci.*, 2019, **18**, 140

Rosindone revisited: a computational and photophysical study of 7-phenylbenzo[*a*]phenazine-5(7*H*)-one (PBP)†

Dumitru Sirbu,[a] Rebecca Wales,[a] David R. Geary,[a] Paul G. Waddell[b] and Andrew C. Benniston *[a]

Received 3rd July 2018,
Accepted 21st October 2018

DOI: 10.1039/c8pp00279g

rsc.li/pps

A reasonable gram quantity of the crystalline red dye 7-phenylbenzo[*a*]phenazine-5(7*H*)-one (**PBP**) was synthesised by the condensation of *N*-phenylbezene-1,2-diamine with 2-hydroxynaphthalene-1,4-dione in acetic acid (58% yield). The molecular structure of the dye, as determined by single-crystal X-ray crystallography, reveals a near planar phenazinone-like core, and an *N*-phenyl group twisted out of this plane by around 85°. The CO bond length of 1.241(2) Å is consistent with double bond character, which supports minor ground state zwitterionic character to the compound. The wavelength maximum for the observed partially structured low-energy absorption band is relatively insensitive to changes in the solvent polarity and polarizability. TD-DFT calculations predict that the long wavelength absorption envelope originates from localised π–π* transitions with no contribution from an n–π* state. The fluorescence quantum yield and singlet lifetime of the dye in MeCN are 0.12 and 3.0 ns, respectively. Fluorescence maxima are slightly sensitive to the solvent and changes in the Stokes shifts for a small series of alkanols were fitted to the Lippert–Mataga equation to afford a change in dipole moment of 8 ± 2 D. Calculations also reveal that full rotation of the *N*-phenyl group is severely restricted in the ground state (ΔE_{GS} = 29 kcal mol^{-1}) and in the first-excited singlet state (ΔE_{ES} = 34 kcal mol^{-1}). The rocking back and forth of the phenyl group distorts the phenazinone-like backbone as it becomes co-planar and a minor solvent viscosity effect was observed in hydrogen bonding alkanol solvents.

Introduction

Rosinduline, or azocarmine G, is a doubly sulfonated water soluble red dye that has been recognised for well over 100 years, and has found numerous applications including the staining of cells for microscopy studies,[1] as a redox titration indicator,[2] a metal ion and poisons detector[3] and a food dye (Fig. 1). Despite the fact that rosinduline is a well-established commercial dye the lack of photophysical and photochemical data on the material is surprising. Most in-depth search results are focussed on rosinduline preparation details or its derivatives[4] and quantitative data are conspicuously absent. Photodegradation of the dye by UV-photo Fenton chemistry,[5] or its photooxidation over hydroxyl iron–aluminium pillared bentonite using hydrogen peroxide[6] would appear to suggest the compound can be degraded. The fundamental core to the dye is primarily based on a phenazinone-like moiety and is identified as 7-phenylbenzo[*a*]phenazine-5(7*H*)-one (**PBP**), or rosindone, as shown in Fig. 1. Again, any specific fundamental data for **PBP** was sparse and whether or not the compound even displayed fluorescence was hard to track down. Whereas oxidation of the dye looked reasonable because of the amine feature, the conjugated carbonyl unit also seemed a facile sight for reduction to a ketyl-like radical. Certainly this latter facet was considered appealing in regard to the use of **PBP** as a photooxidant, providing the compound performed in a similar manner to H-abstraction agents such as benzophenone.[7] Noting the photoxidant capability of benzophenone is primarily driven from its triplet n–π* state,[8] the practical question of what the energy level diagram for **PBP** resembled seemed pertinent. Hence, given the lack of quality data for **PBP** a detailed photophysical investigation of the compound was undertaken coupled to a predictive DFT computational study. The dye exhibits modest fluorescence in MeCN with a quantum yield of 0.12. Identification of the triplet state and its quantum yield was problematic pointing to poor intersystem crossing of the singlet and triplet states. This observation is attributed to the

[a]*Molecular Photonics Laboratory, Chemistry-School of Natural and Environmental Sciences, Newcastle University, Newcastle upon Tyne, NE1 7RU, UK. E-mail: andrew.benniston@ncl.ac.uk*

[b]*Crystallography Laboratory, Chemistry-School of Natural and Environmental Sciences, Newcastle University, Newcastle upon Tyne, NE1 7RU, UK*

†Electronic supplementary information (ESI) available: Computational calculations, deconvoluted spectrum, crystal packing diagram, additional graphs and NMR spectra. CCDC 1852962. For ESI and crystallographic data in CIF or other electronic format see DOI: 10.1039/c8pp00279g

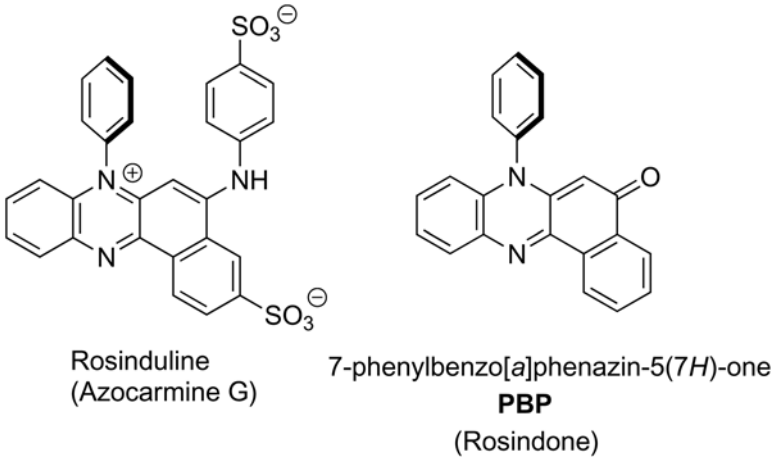

Fig. 1 The chemical structure of rosinduline (left) and the basic starting material core 7-phenylbenzo[*a*]phenazine-5(7*H*)-one (**PBP**) (right).

spin and orbitally forbidden intersystem crossing of the first-excited singlet (S_1) π–π* state to the near isoenergetic second-excited triplet (T_2) π–π* state. The low fluorescence quantum yield is somewhat linked to the moderately efficient non-radiative deactivation of S_1 caused by distortion of the phenazinone-like backbone facilitated by rocking of the *N*-phenyl group.

Results and discussion

Synthesis and characterisation

The title compound 7-phenylbenzo[*a*]phenazine-5(7*H*)-one (**PBP**) was synthesised in an unoptimised yield of 58% by the condensation of *N*-phenylbezene-1,2-diamine with 2-hydroxy-naphthalene-1,4-dione in acetic acid and precipitation. Despite the modest yield the compound can be prepared on a multi-gram scale. The crude dark red solid, as evidenced by ^{1}H NMR spectroscopic analysis, was around 95% pure but further purification by recrystallization afforded a red crystalline material. Both ^{1}H and ^{13}C NMR spectra were fully consistent with the structure, and the modest band at 1613 cm^{-1} in the FT-IR spectrum confirmed the presence of the carbonyl unit. The dye is soluble, to various degrees, in most organic protic and aprotic solvents at room temperature, but it is completely insoluble in water. Single crystals of **PBP** grown from a chloroform/hexane solution by slow evaporation were of suitable quality for an X-ray structure determination, and the molecular structure is illustrated in Fig. 2. Selected bond lengths and angles are shown in Table 1. Considering the structure of **PBP** some degree of zwitterionic character might be expected, so as to generate more single bond character in the carbonyl subunit (eqn (1))

(1)

The O1–C7 bond length is certainly more in fitting with formal double bond character and this, coupled with the quinoidal bond length pattern of the C7–C8–C9–C10–C11–C12

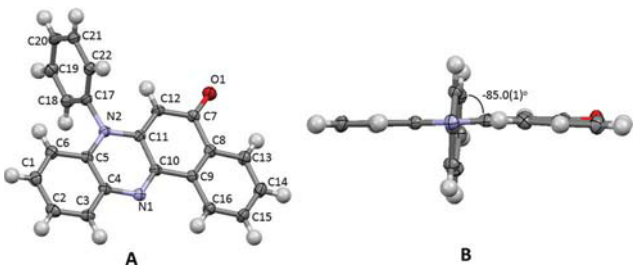

Fig. 2 Crystal structure of **PBP** with ellipsoids drawn at the 30% probability level highlighting the atomic numbering scheme (A), and the view down the N1–N2 axis to show the twist of the *N*-phenyl subunit and the near planarity of the phenazinone-like group.

Table 1 Selected bond lengths and angles for the X-ray crystal structure of **PBP**

Atoms	Bond length[a]/Å	Atoms	Bond angle[a] /°
O1–C7	1.241(2) (1.231)	O1–C7–C8	120.39(11) (121.03)
N1–C4	1.381(2) (1.376)	O1–C7–C12	122.31(11) (121.96)
N1–C10	1.304(2) (1.299)	N2–C11–C12	122.69(11) (122.80)
N2–C5	1.390(2) (1.394)	C4–N1–C10	118.86(10) (119.80)
N2–C11	1.380(2) (1.393)	C5–N2–C11	121.96(10) (121.60)
N2–C17	1.451(2) (1.443)	C11–N2–C17	117.86(10) (119.02)
C7–C12	1.431(2) (1.447)	C5–N2–C17	120.08(10) (119.38)
C11–C12	1.368(2) (1.368)		
C7–C8	1.491(2) (1.494)		

[a] DFT calculated bond lengths and angles given in brackets for the gas phase structure of **PBP** as determined using Gaussian 09 (B3LYP) and a 6-311G+(d) basis set.[9]

ring and the comparable N2–C11/N2–C5 bond lengths, would suggest there is little ground-state zwitterionic character. The short N1–C10 bond is also as expected for a phenazinone-based ring. The phenazinone-like unit is almost planar with a root mean square deviation of 0.060 Å (Fig. 2B), though a small deviation from planarity is observed in the C8–C9–C13–C14–C15–C16 ring, which is folded *ca.* 1.4° towards the adjacent quinoidal ring. The *N*-phenyl group is as might be expected twisted out of plane by 85° (torsion angle C11–N2–C17–C22) to alleviate unfavourable H–H steric interactions. There are no exceptional crystal packing features.

Molecular modelling and predictions

The gas-phase structure for **PBP** as calculated using DFT (B3LYP) and a 6-311G+(d) basis set is in fairly good agreement with the X-ray crystal structure; calculated bond lengths and angles (Table 1) are in some cases well within 3σ. The *N*-phenyl twist angle is 89.9° (*cf.* 85° for the X-ray structure). The HOMO is almost exclusively localized on the phenazinone-like moiety with notable electron density residing along the C1–C6–C5–N2–C11–C12–C7–O1 backbone. In comparison the LUMO is more uniformly distributed over the entire molecular framework including the C8–C9–C13–C14–C15–C16 aromatic ring. The charge distribution within the molecular scaffold is manifest in a modest ground-state dipole moment of 5.6 D. Calculated ground-state dipole moments for **PBP** immersed in a solvent matrix using an integral equation formalism polarizable continuum model (IEFPCM) with various dielectric constants displayed modest alterations (see ESI†). The longest wavelength absorption maximum (λ_{max}) calculated for the gas phase structure using a time-dependent DFT (TD-DFT) approach is located at 463 nm, and shifts to 475 (2.61 eV) when the molecule is fully immersed in a MeCN solvent bath. The major contribution to the absorption envelop arises from the HOMO to LUMO electronic transition (see ESI†) which is essentially π–π*. There is no indication of an n–π* transition contributing to the long wavelength absorption envelope. Other calculated values of λ_{max} for solvents of diverse polarity do not vary by more than 2 nm, which would suggest that solvent interactions with **PBP** do not affect the energy of electronic transitions to any major extent. Comparison of the TD-DFT calculated first-excited singlet state and ground-state structures in a MeCN solvent bath reveals that the molecule remains planar, but the zwitterionic character perturbs bond lengths of the central diazo ring and the keto-ene containing ring (see ESI†). The structural change is accompanied by a small change in the dipole moment (0.8 D) (Fig. 3).

Calculated energies for the triplet states of **PBP** are enlightening in as much that the lowest-energy triplet state (T_1) is located at *ca.* 1.7 eV, and is associated with unpaired electrons in a π–π* state. A higher lying triplet π–π* (T_2) state at around 2.5 eV is very close in energy to the S_1 state (2.6 eV). We might expect that any S_1 to T_2 intersystem crossing, despite the small energy gap, to be slow since the transition is both spin and orbitally forbidden (El Sayed's Rule[10]). Intersystem crossing S_1 to T_1 is also likely to be slow based on a similar argument and

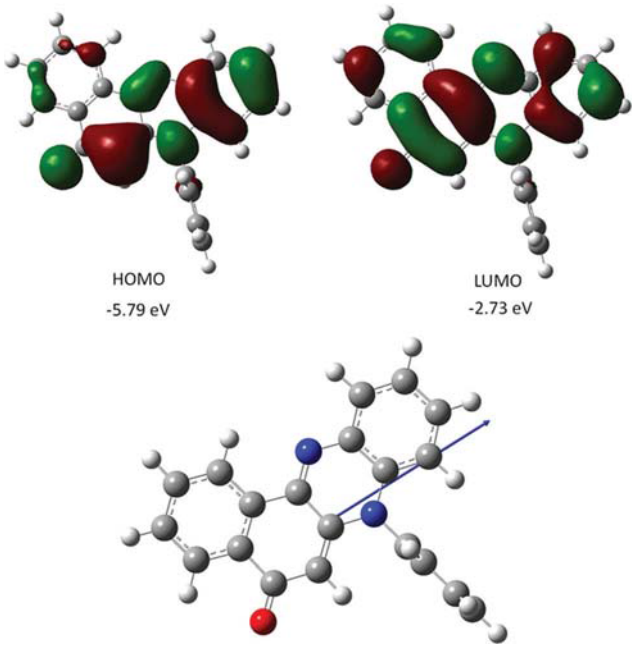

Fig. 3 Representation of selected DFT calculated Kohn–Sham frontier molecular orbitals for **PBP** (top), and the calculated ground-state structure showing the direction of the dipole moment (bottom).

the large energy gap. Of course, the T_2 to T_1 transition is both spin and orbitally allowed which might presuppose fast interconversion, but it is noted that considerable energy must be dissipated during the process. Given the probable small reorganisation that would accompany the transition, the rate for such a non-radiative process might be actually slower than expected (energy gap law[11]).

Focussing on the *N*-phenyl as a conceivable rotor subunit within the structure, potential energy calculations using Gaussian 09[9] (B3LYP, 6-311G+(d)) were performed on the gas-phase ground-state structure as the phenyl group was rotated through 360° (Fig. 4). The phenyl unit becomes more aligned with the phenazinone-like ring as the dihedral angle approaches zero, which causes the group to bow and lose planarity (see ESI†).[12] In an extreme conformation the nitrogen atom at the *N*-phenyl takes on more of a pyramidal feature. The energy barrier to full rotation of *ca.* 29 kcal mol^{-1} (121 kJ mol^{-1}) is substantial and on par with hindered rotation of the phenyl group in methaqualone and mecloqualone.[13] Complementary TD-DFT potential energy calculations performed on the first excited-state structure reveal that the barrier to rotation is still significant (*ca.* 34 kcal mol^{-1}). Based on these calculations no so-termed molecular rotor effect[14] would be expected, such that viscosity of the surrounding medium should not affect localised fluorescence to any great extent.

Electrochemistry

Cyclic voltammetry performed on **PBP** in dry N_2-purged MeCN (0.2 M TBATFB background electrolyte) revealed a straightforward redox chemistry in both the oxidation and reduction

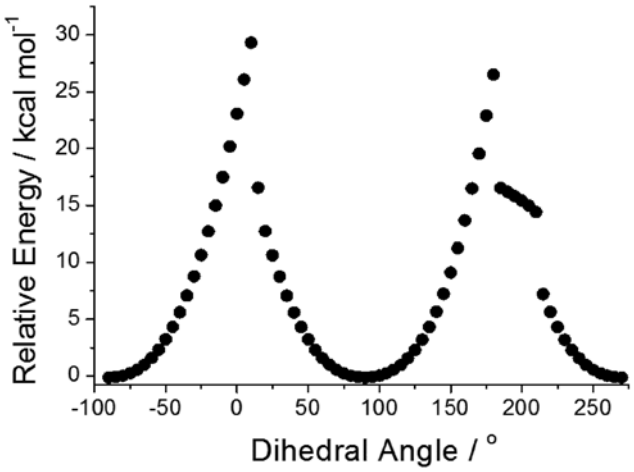

Fig. 4 Relative energies of **PBP** in the ground state *versus* the dihedral angle at the *N*-phenyl subunit. Each point represents a change in angle of 5°.

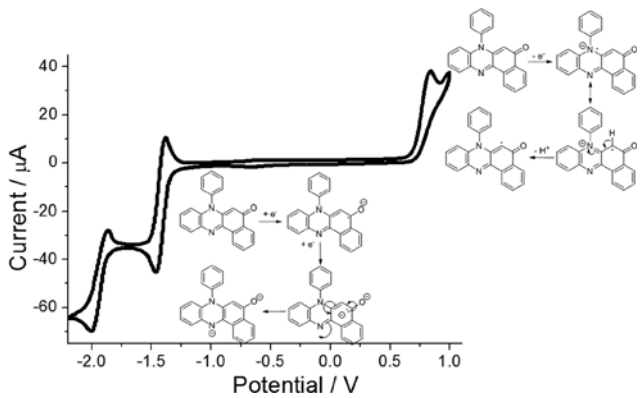

Fig. 5 Cyclic voltammogram recorded for **PBP** at a glassy carbon working electrode in N_2-purged dry MeCN containing 0.2 M TBATFB background electrolyte. Counter electrode = platinum wire, scan rate = 50 mV s^{-1}, reference electrode = $Ag/AgNO_3$ in MeCN, internal reference = Fc^+/Fc (+0.09 V). Insert shows plausible products from one electron oxidation and sequential one electron reduction of the compound.

segments of the voltammogram (Fig. 5). Scanning to oxidative potentials produced an irreversible wave located at E_1 = +0.83 *vs.* Fc^+/Fc which is taken to be removal of an electron from the HOMO. The irreversibility of the wave is correlated to breakdown of the cation radical, possibly the result of deprotonation at the aromatic ring and then dimerization or solvent addition. Upon reductive scanning a reversible wave was seen at E_2 = −1.43 V (ΔE = 60 mV) *vs.* Fc^+/Fc which corresponds to radical anion formation at the carbonyl group. Further scanning produced a quasi-reversible wave at E_3 = −1.94 V (ΔE = 130 mV) *vs.* Fc^+/Fc and is associated with dianion formation. The major peak separation E_2–E_3 of *ca.* 0.5 V likely arises from the unfavourable electrostatic repulsion created by addition of an electron to the anion radical, since protons are lacking in the dry solvent to neutralise the charge. The energy gap E_1–E_2 of *ca.* 2.2 eV is considerably smaller than the DFT calculated HOMO–LUMO energy gap (3.05 eV) which is not uncommon, and similar findings were reported previously for other unrelated molecular systems.[15]

Spectroscopic studies

The representative electronic absorption spectrum for **PBP** in MeCN is illustrated in Fig. 6. The lowest energy absorption envelope is partly structured comprising of two clear peaks located at 475 nm, 498 nm and a partial shoulder at *ca.* 527 nm. There is also sign of an additional shoulder at the short wavelength side of the absorption band. The deconvoluted absorption envelope using five constant half-width Gaussian profiles (fwhm = 1317 cm^{-1}) locates this high energy band at 440 nm (see ESI†). The molar absorption coefficient (ε_{max}) measured at 498 nm is 13 000 mol^{-1} dm^3 cm^{-1} corresponding to an oscillator strength (f) of 0.17. It is worth noting that DFT calculations suggest the absorption profile comprises primarily of a π–π* electronic transition. Below 400 nm the absorption profile is dominated by two sharp peaks located at 309 nm and 255 nm. Absorption spectra recorded for **PBP** in solvents of various polarity and polarizability were essentially similar in appearance and only minor changes (*ca.* 6 nm) were observed in peak maxima; the overall effect was satisfactorily predicted from the TD-DFT calculations.

Red emission from a dilute MeCN solution of **PBP** is evident even by eye upon UV excitation. The collected excitation independent low-energy fluorescence spectrum does not mirror perfectly the absorption profile, but it is partially structured with peaks located at 575 nm and 613 nm (Fig. 6). A broad tail to the emission stretches to around 800 nm. The crossing point of the normalised absorption and fluorescence spectra is located at 548 nm (2.26 eV). The Stokes' shift (SS) of 2689 cm^{-1}, calculated from the difference between the absorption and fluorescence maxima, does suggest that there is displacement along the reaction coordinate for the ground- and excited-state potential energy surfaces. The partial structured nature of the absorption spectrum is consistent with

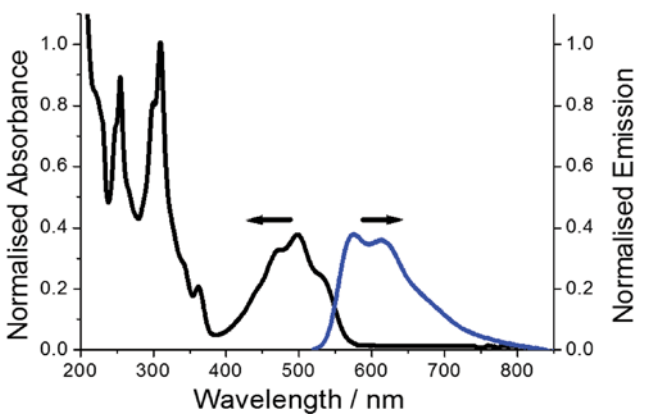

Fig. 6 Normalised absorption profile (black) for **PBP** and fluorescence spectrum (blue) in dilute MeCN. Excitation wavelength = 490 nm.

Berlman's protocol[16] that the ground state is planar. DFT calculations suggest that alterations in bond-lengths within the phenazinone-like molecular framework occur upon formation of the first-excited state but it essentially remains planar. The partial structured nature of the emission profile is consistent with this notion, but the major reorganisation is likely related to rocking of the *N*-phenyl group. This latter idea was supported by a variable low-temperature study in EtOH in which fluorescence spectra were recorded from 290 K to 80 K. Between 290 K and 160 K where the EtOH remained fluidic the ϕ_{FLU} steadily increased and was analysed in terms of the Arrhenius equation (see ESI†). The small ΔE of only 3 kJ mol^{-1} supports a weakly activated process consistent with libration of the phenyl group. It is also noted that at the glass transition temperature of EtOH (*ca.* 100 K) the ϕ_{FLU} increased significantly as molecular motions were curtailed in the solid glass. In addition, the SS at 80 K reduced significantly to 428 cm^{-1}.

Fluorescence excitation spectra recorded at disparate emission wavelengths are an acceptable match to the absorption profile. The fluorescence quantum yield (ϕ_{FLU}) of 0.12 is rather modest, and fluorescence decays were strictly mono-exponential at all monitoring wavelengths to afford a singlet lifetime (τ_S) of 3.0 ns. The radiative decay constant (k_{RAD}) calculated using the Strickler–Berg expression[17] of 1.1×10^8 s^{-1} is considerably larger (*ca.* 3 fold) than the measured value of 4×10^7 s^{-1} ($k_{RAD} = \phi_{FLU}/\tau_S$). Such a disparity is not too surprising considering the assumption of a small structural alteration in the Strickler–Berg model and the displaced potential energy surfaces for **PBP**. Non radiative decay is clearly dominant in deactivation of the first-excited singlet state, the measured non-radiative decay constant ($k_{NR} = 1/\tau_S - k_{RAD}$) is 2.9×10^8 s^{-1}.

In an attempt to try and shed more light onto the efficiency of intersystem crossing and the nature of the triplet states nanosecond flash photolysis experiments were performed. Excitation of a sample of **PBP** in N_2-purged MeCN with a 10 ns laser pulse delivered at 532 nm produced clear ground-state bleaching at around 500 nm, and a weak transient profile centred at 800 nm (Fig. 7). A major problem was the rapid degradation of the sample after repetitive laser excitation shots. An acceptable fit to the transient signals at 800 nm to a single exponential was possible to afford a lifetime of 16 μs. A similar experiment performed with addition of a heavy atom perturber to the solution (10% EtI) did result in a slight signal enhancement to the long wavelength profile; the introduction of oxygen into the solution resulted in its complete removal of the signal. Based on these findings the long wavelength transient signal is assigned to the T_1–T_n absorption spectrum.

Very weak partially structured phosphorescence was observed at around 12 790 cm^{-1} (1.6 eV) from an ethanol glass containing **PBP** at 80 K (see ESI†). The calculated energy of the triplet (*ca.* 1.7 eV) is remarkably similar to this value but some caution is noted: the phosphorescence spectrum shape was not dependable over several runs and the measured intensity was very low. The difficulty in collecting a clear phosphorescence spectrum is consistent with poor intersystem crossing.[18]

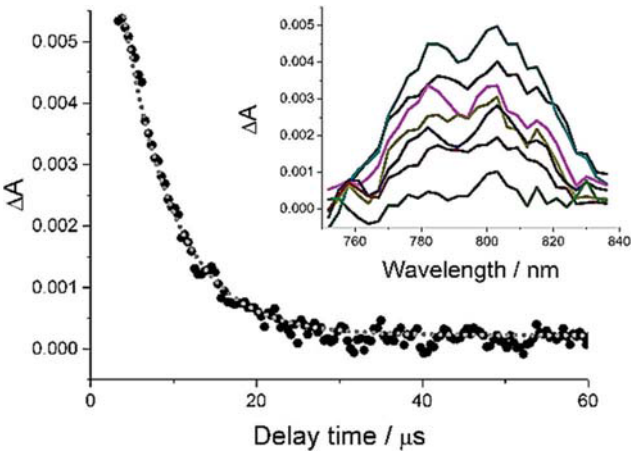

Fig. 7 Transient spectra recorded at 800 nm after excitation of a sample of **PBP** in N_2-purged MeCN with a 10 ns laser pulse delivered at 532 nm.

Fluorescence measurements in various solvents

No distinct dependence of ϕ_{FLU} with solvent viscosity was anticipated as established by the phenyl rotation computational calculations and predictions. The envisaged modest change in the dipole moment upon the ground-state to first-excited state transition also hinted at limited dependency of the Stokes' shift (SS) with solvent polarity. Hence, fluorescence spectra were recorded in a small range of alkanol and aprotic solvents and the results are collected in Table 2. Given the presence of a carbonyl group within **PBP** intermolecular hydrogen bonding was likely to be integrated into any overall solvent effect in the alkanol series. The change in solvent from methanol to pentan-1-ol is accompanied by a modest increase in ϕ_{FLU}, but essentially values plateau across the series. Analysis of the alterations in ϕ_{FLU} in terms of the Förster–Hoffmann[19] equation produced an adequate linear relationship (see ESI†), but the modest slope (α = 0.13) suggests a weak viscosity dependency as predicted. Presumably the rocking back and forth of the phenyl subunit and the distortion it causes in the phenazinone, coupled to solvent hydrogen bonding to the carbonyl is just sufficient to produce the effect.[20] The variation of ϕ_{FLU} within the solvent series is also worth noting in terms of the dielectric constant (ε) (see ESI†). The high ϕ_{FLU} are generally associated with the low polarity solvents. A focus on the linear alkanols again demonstrates that the ϕ_{FLU} reaches a limiting value of *ca.* 11%. The destabilisation of the excited state in the low polarity alkanols is presumably sufficient to reduce the rate of non-radiative decay in line with the energy-gap law.[11] An interesting result is seen for the diol ethylene glycol which is highly viscous with a concomitant high ε, but **PBP** has a low ϕ_{FLU} in the solvent. The potential hydrogen-bonding viscosity enhancement is suppressed by a polarity effect. The highest ϕ_{FLU} observed in toluene can be attributed to two factors; namely, the low polarity of the solvent and high refractive index since $k_{RAD} \propto n^2$ (Strickler–Berg equation).[17]

Table 2 Selected photophysical properties of **PBP** in various solvents at 22 °C

Solvent	ε^a	n^b	η^c (cP)	$\lambda_{MAX}{}^d$ (cm^{-1})	$\lambda_{FLU}{}^e$ (cm^{-1})	SS (cm^{-1})	ϕ_{FLU}
MeOH	32.6	1.327	0.54	19 960	17 422	2538	0.070
EtOH	24.6	1.360	0.69	19 920	17 668	2252	0.094
Propan-1-ol	20.5	1.384	1.95	19 960	17 606	2354	0.105
Butan-1-ol	17.5	1.397	2.54	20 000	17 637	2363	0.108
Pentan-1-ol	13.9	1.407	3.62	19 920	17 637	2283	0.113
Hexan-1-ol	13.3	1.414	4.58	19 881	17 699	2182	0.110
Heptan-1-ol	12.1	1.424	5.81	19 920	17 668	2252	0.110
Octan-1-ol	10.3	1.429	7.29	19 920	17 730	2190	0.113
Nonan-1-ol	8.83	1.433	8.97	19 881	17 762	2119	0.124
Decan-1-ol	7.2	1.435	12.0	19 881	17 762	2119	0.110
Ethylene glycol	37.7	1.431	16.9	19 841	17 241	2600	0.064
Toluene	2.38	1.496	0.59	20 000	17 668	2332	0.160
MeCN	37.5	1.344	0.33	20 080	17 391	2689	0.120
DCM[f]	8.93	1.421	0.41	19 841	17 483	2358	0.126
THF[g]	7.58	1.405	0.48	19 841	17 606	2235	0.100
EA[h]	6.02	1.370	0.46	20 000	17 575	2425	0.090
$CHCl_3$	4.81	1.443	0.54	19 920	17 606	2314	0.144
Et_2O	4.33	1.350	0.22	20 040	17 889	2151	0.113

[a] Dielectric constant (ref. 23). [b] Refractive index. [c] Bulk solvent viscosity. [d] Absorption wavelength maximum. [e] Corrected fluorescence wavelength maximum. [f] Dichloromethane. [g] Tetrahydrofuran. [h] Ethyl acetate.

The change in the SS for the entire solvent series, as analysed using the Lippert–Mataga equation[21] (eqn (2)), was limited, but again a focus on the alkanols provided a clear dependency with the solvent function (ΔF) as shown in Fig. 8. The difference in dipole moment of 8 ± 2 D using a = 5.8 Å is again indicative of only partial increased transfer of charge upon excitation.

$$\mathrm{SS} = 10\,068\left[\frac{(\mu_{es}-\mu_{gs})^2}{a^3}\right]\Delta F + C$$
$$\Delta F = \left[\frac{\varepsilon-1}{2\varepsilon+1} - \frac{n^2-1}{2n^2+1}\right] \quad (2)$$

Here a (in Å) represents the radius of the spherical cavity in which the molecule resides and is provided by a solvent dielectric continuum, and the difference between the ground and excited state dipole moments ($\mu_{es} - \mu_{gs}$) is in Debye.[22]

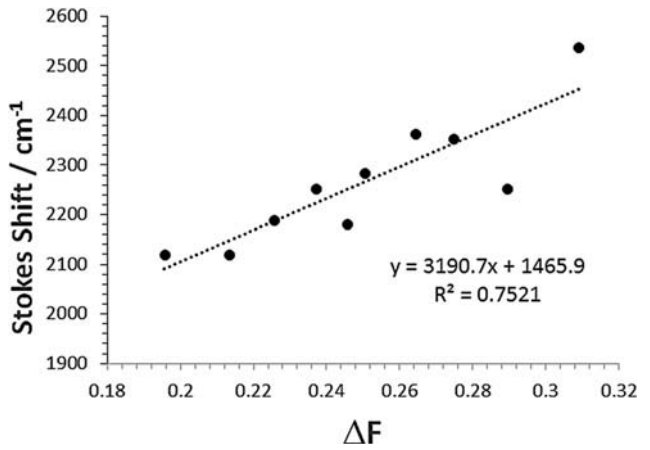

Fig. 8 Relationship between Stokes shift (SS) and the solvent Pekar function ΔF for the linear mono-protic alkanol series. The linear equation and goodness-of-fit is shown in the insert.

Conclusions

Using a one-pot reaction it is straightforward to prepare multigram quantities of the red fluorescent dye 7-phenylbenzo[*a*]phenazine-5(7*H*)-one. The interaction of mono-protic hydrogen bonding solvents at the carbonyl group coupled to rocking of the *N*-phenyl group is important in influencing the level of fluorescence from the dye. However, the small increase in the ϕ_{FLU} for a *ca.* 20-fold increase in solvent viscosity rules out the usefulness of the dye as a fluorescent rheology probe. There appears no clear way to drastically enhance the fluorescence viscosity response since there is also a prominent polarity effect which can dominate in solvents with a low dielectric constant. The dye does however contain several sites for further functionalisation or modification which could perturb the excited state properties in a positive manner. Preliminary findings have shown that nucleophiles add adjacent to the *N*-phenyl group in a reaction similar to Michael addition to an α,β unsaturated ketone. New molecular systems are in development based on this finding, especially chiral dimers that facilitate exciton coupling and exhibit polarised luminescence. Considering the *N*-phenyl group in **PBP** does play a pivotal role in excited state deactivation its removal may also have a positive effect.

Experimental

^{1}H and ^{13}C NMR spectra were recorded on a Bruker 700 MHz spectrometer. FT-IR spectrum was recorded on a PerkinElmer FT-IR Spectrum Two spectrometer. Absorption spectra were

obtained using a Shimadzu UV-1800 spectrophotometer. Corrected emission and excitation spectra were obtained using a Shimadzu RF-6000 spectrofluorophotometer. The spectra were not corrected again to take into account that bandpass in wavenumbers is not constant when the spectrum is recorded in constant wavelength resolution by using $I(\tilde{\nu}) = \lambda^2 I(\lambda)$. Quantum yields were calculated using Rhodamine 6G (ϕ_{FLU} = 0.95 EtOH)[24] as a standard and by the comparison method, and the fluorescence lifetime was measured using a PTI EasyLife apparatus. Nanosecond flash photolysis experiments were carried out using an Applied Photophysics LKS50 instrument.

Crystal structure data for **PBP** were collected at 150 K on a Xcalibur, Atlas, Gemini ultra-diffractometer equipped with a fine-focus sealed X-ray tube (λ CuK_α = 1.54184 Å) and an Oxford Cryosystems CryostreamPlus open-flow N_2 cooling device. Cell refinement, data collection and data reduction were undertaken *via* the software CrysAlisPro (Rigaku OD, 2015). An analytical numeric absorption correction was applied to the intensities using a multifaceted crystal model based on expressions derived by Clark & Reid.[25] The structure was solved using ShelXT (Sheldrick, 2015)[26] and refined by XL (Sheldrick, 2008).[27] All non-hydrogen atoms were refined as anisotropic and hydrogen atoms were place with idealised geometry and U_{iso} set to 1.2 times that of the parent atom.

Computational calculations were performed using a 32-bit version of Gaussian09 on a quadruple-core Intel Xeon system with 4GB RAM. The calculations were run in parallel, fully utilising the multi-core processor. To reduce computational time low-level calculations were carried out to minimise structures using Hartree–Fock and a low basis set. Energy-minimised structures were then used to feed high-level density functional theory (DFT) calculations starting firstly with B3LYP and the 3-21G basis set. The complexity of the basis set was increased and results from calculations compared. The 6-311G+(d) basis set was deemed sufficient for comparison purposes. Calculations in a solvent medium were carried out using the integral equation formalism polarization continuum model (IEFPCM). Phenyl rotation calculations were performed in Gaussian 09 using DFT and the scan method with the relaxed potential energy surface option where geometry optimization at each step was carried out while maintaining the scanned variable constant. Excited-state calculations were performed using the time-dependent DFT method. Calculations during refinement were monitored using the program Molden and by visualising the geometrical convergence at each step.

Preparation of PBP

A 50 ml two-necked round-bottom flask was charged with 2-hydroxy-1,4-naphthoquinone (3.48 g, 20 mmol,) and *N*-phenylene-*o*-phenylenediamine (3.69 g, 20 mmol,) which was then purged with nitrogen. N_2-purged glacial acetic acid (100 ml) was added and the reaction mixture was stirred for 60 minutes at room temperature. The temperature was raised to 60 °C and then stirred for a further 60 minutes. The reaction mixture was left to cool and a TLC was taken (95 : 5, DCM : methanol) to check the extent of the reaction. The mixture was then added to distilled water and the crimson red precipitate filtered through a Büchner funnel. The solid was washed with water to remove residual acetic acid followed by diethyl ether to remove the unreacted materials. The product was dried overnight under vacuum and by NMR spectroscopy was *ca.* 95% pure. The sample was purified by recrystallisation from ethanol and water to give a red microcrystalline solid. Yield: 3.7 g, 11.5 mmol, 58%. Mp 263–265 °C. FT-IR (cm^{-1}) 749 (s), 776 (m), 830 (m), 856 (w), 949 (w), 1000 (w), 1030 (w), 1120 (w), 1131 (w), 1157 (w), 1244 (s), 1310 (s), 1355 (w), 1454 (w), 1473 (s), 1536 (s), 1587 (s), 1614 (w), 3063 (w). ^{1}H NMR ($CDCl_3$, 700 MHz) δ 8.99 (dd, 1H, J = 7.8 Hz, J = 1.1 Hz), 8.37 (dd, 1H, J = 7.6 Hz, J = 1.2 Hz), 8.05–8.08 (m, 1H), 7.76–7.82 (m, 2H), 7.72 (tt, 2H, J = 7.8 Hz, J = 1.9 Hz), 7.65 (tt, 1H, J = 7.6 Hz, J = 1.3 Hz), 7.37–7.40 (m, 2H), 7.33–7.35 (m, 2H), 6.67–6.70 (m, 1H), 5.61 (s, 1H). ^{13}C NMR ($CDCl_3$, 176 MHz) δ 182.0, 147.4, 140.9, 137.0, 134.8, 133.1, 132.8, 131.9, 131.7, 131.5, 131.1, 131.0, 130.6, 130.4, 128.5, 125.6, 125.1, 124.1, 115.3, 101.1. HRMS nanoESI m/z calculated for $C_{22}H_{15}N_2O$ 323.1179, found 323.1184 $[M + H]^+$.

Conflicts of interest

There are no conflicts to declare.

Acknowledgements

We thank the EPSRC sponsored mass spectrometry service at Swansea for collecting mass spectra and Newcastle University for financial support. Dr Joshua Karlsson is thanked for help in the nanosecond flash photolysis experiments.

References

1 S. Hayashi, T. Takamatsu and S. Fujita, Cytofluorometric nuclear-DNA determinations on the atrioventricular nodel cells in human hearts, *Histochemistry*, 1986, **85**, 111.
2 L. Michaelis, Rosinduline as oxidation-reduction indicator, *J. Biol. Chem.*, 1931, **91**, 369.
3 S. Abbasi, H. Barzegaramiri and A. Farmany, Determination of trace amounts of silver(I) in the presence of an activator with a kinetic method, *Rare Met.*, 2014, **33**, 731; H.-Y. Wang, Special analysis of dissolved copper in wastewater with azocarmine B by light absorption ratio variation combined with continuous analysis, *J. Chin. Chem. Soc.*, 2008, **55**, 1338.
4 O. Fischer and E. Hepp, The induline group, *Liebigs Ann. Chem.*, 1891, **262**, 237.
5 T. Xu, Y. Liu, F. Ge and Y. Ouyang, Application of surface methodology for optimization of azocarmine B removal by photo-Fenton process using hydroxyl-iron-aluminium bentonite, *Appl. Surf. Sci.*, 2013, **280**, 926.

6 T. Xu, Y. Liu, F. Ge and Y. Ouyang, Simulated solar light photooxidation of azocarmine B over hydroxyl iron-aluminium pillared bentonite, *Appl. Clay Sci.*, 2014, **100**, 35.

7 G. Dormán, H. Nakamura, A. Pulsipher and G. D. Prestwich, The life of pi-star: Exploring the exciting and forbidden worlds of the benzophenone photophore, *Chem. Rev.*, 2016, **116**, 15284.

8 G. Dormán and G. D. Prestwich, Benzophenone photophores in biochemistry, *Biochemistry*, 1994, **33**, 5661.

9 M. J. Frisch, G. W. Trucks, H. B. Schlegel, G. E. Scuseria, M. A. Robb, J. R. Cheeseman, G. Scalmani, V. Barone, B. Mennucci, G. A. Petersson, H. Nakatsuji, M. Caricato, X. Li, H. P. Hratchian, A. F. Izmaylov, J. Bloino, G. Zheng, J. L. Sonnenberg, M. Hada, M. Ehara, K. Toyota, R. Fukuda, J. Hasegawa, M. Ishida, T. Nakajima, Y. Honda, O. Kitao, H. Nakai, T. Vreven, J. A. Montgomery, Jr., J. E. Peralta, F. Ogliaro, M. Bearpark, J. J. Heyd, E. Brothers, K. N. Kudin, V. N. Staroverov, T. Keith, R. Kobayashi, J. Normand, K. Raghavachari, A. Rendell, J. C. Burant, S. S. Iyengar, J. Tomasi, M. Cossi, N. Rega, J. M. Millam, M. Klene, J. E. Knox, J. B. Cross, V. Bakken, C. Adamo, J. Jaramillo, R. Gomperts, R. E. Stratmann, O. Yazyev, A. J. Austin, R. Cammi, C. Pomelli, J. W. Ochterski, R. L. Martin, K. Morokuma, V. G. Zakrzewski, G. A. Voth, P. Salvador, J. J. Dannenberg, S. Dapprich, A. D. Daniels, O. Farkas, J. B. Foresman, J. V. Ortiz, J. Cioslowski and D. J. Fox, *Gaussian 09, Revision D.01*, Gaussian, Inc., Wallingford CT, 2013.

10 M. A. El-Sayed, Triplet state. Its radiative and non radiative properties, *Acc. Chem. Res.*, 1968, **1**, 8.

11 R. Englman and J. Jortner, Energy gap law for radiationless transitions in large molecules, *Mol. Phys.*, 1970, **18**, 145.

12 The hysteresis and shoulder seen in the figure may be explained by the fact that at the point where the *N*-phenyl group adopts a pyramidal geometry it can point up or down. The bowing of the structure need not be identical for the two cases leading to a loss of mirror symmetry between the two conformations. Semi-empirical calculations (AM1) performed on the ground- and excited-state structures showed the same effect albeit with slightly different energies to the rotation barriers (see ESI†). The barrier to rotation in the excited state was still around 5 kcal mol^{-1} larger than in the ground state and identical to the value from the DFT calculations. There are limitations to the method of using a single-coordinate in driving the energy minimization at each step change. The energy minimized structure may get trapped in a valley on the potential energy surface and not be able to "slip" to another structure. It is noted that the shoulder observed is not reproduced in a simple MM^{+} calculation, but the barrier to rotation is still significant (24 kcal mol^{-1}).

13 E. Azanli, R. Rothchild and A.-M. Sapse, Ab-initio studies of hindered aryl rotations of methaqualone, mecloqualone and 3-(2,6-difluorophenyl)-2-methyl-4(3H)-quinazolinone, *Spectrosc. Lett.*, 2002, **35**, 257.

14 R. A. Loutfy and B. A. Arnold, Effect of viscosity and temperature on torsional relaxation of molecular rotors, *J. Phys. Chem.*, 1982, **86**, 4205.

15 J. Conradie, A frontier orbital energy approach to redox potentials, *J. Phys.: Conf. Ser.*, 2015, **633**, 012045.

16 I. B. Berlman, On an empirical correlation between nuclear conformation and certain fluorescence and absorption characteristics of aromatic compounds, *J. Phys. Chem.*, 1970, **74**, 3085.

17 S. J. Strickler and R. A. Berg, Relationship between absorption intensity and fluorescence lifetime of molecules, *J. Chem. Phys.*, 1962, **37**, 814.

18 At 80 K in EtOH the ϕ_{FLU} is *ca.* 60% meaning the quantum yield of intersystem crossing (ϕ_{ISC}) plus the quantum yield for internal conversion (ϕ_{IC}) is about 40%. From comparison of the fluorescence area to the phosphorescence area at 80 K the ϕ_{ISC} is only at best 1%.

19 T. Förster and G. Hoffmann, Viscosity dependence of fluorescent quantum yields of some dye systems, *Z. Phys. Chem.*, 1971, **75**, 63.

20 G. B. Dutt, Rotational dynamics of nondipolar probes in alkane-alkanol mixtures: Microscopic friction on hydrogen bonding and nonhydrogen bonding solute molecules, *J. Chem. Phys.*, 2000, **113**, 11154.

21 E. Z. Lippert, Dipolmoment und electronenstruktur von angeregten molekülen, *Naturforscher*, 1955, **10a**, 541; N. Mataga, Y. Kaifu and M. Koizumi, Solvent effects upon fluorescence spectra and the dipole moments of excited molecules, *Bull. Chem. Soc. Jpn.*, 1956, **29**, 465.

22 The equation is more commonly written containing several terms including Planck's constant (h), speed of light (c) and the permittivity of free space (ε_0). The terms and corrections for the units are all collected in the 10 068 number for simplicity. The equation can also be rewritten as $\mu_{es} - \mu_{gs} = 0.010\sqrt{ma^3}$ where m is the slope of the Lippert–Mataga plot (see ref. 21).

23 A. R. Maryott and E. R. Smith, *Table of dielectric constants of pure liquids*, U.S. Govt. Print. Off., 1951.

24 A. M. Brouwer, Standards of photoluminescence quantum yields in solution, *Pure Appl. Chem.*, 2011, **83**, 2213.

25 R. C. Clark and J. S. Reid, The analytical calculation of absorption in multifaceted crystals, *Acta Crystallogr., Sect. A: Found. Crystallogr.*, 1995, **51**, 887.

26 G. M. Sheldrick, SHELXT-integrated space-group and crystal structure determination, *Acta Crystallogr., Sect. A: Found. Adv.*, 2015, **71**, 3.

27 G. M. Sheldrick, A short history of SHELX, *Acta Crystallogr., Sect. A: Found. Crystallogr.*, 2008, **64**, 112.